Electronic Supplementary Information (ESI)

Intramolecular charge transfer ampholytes with water-induced pendulum-type fluorescence variation

Xiao-Bin Dong,‡[a] Ling Chen,‡[a] Mei Pan,[c] Wen-Jie Huang,[a] Hua Xiang,[d] Hai-Ping Wang,[a] Zong-Wen Mo,[a] Jia-Wen Ye,*[abe] Kun Zhang[abe] and Xiao-Ming Chen[ac]

[a] School of Biotechnology and Health Science, Wuyi University, Jiangmen 529020, PR China. E-mail: wyuchemyjw@126.com.
[b] International Healthcare Innovation Institute (Jiangmen), Guangdong, PR China.
[c] MOE Key Laboratory of Bioinorganic and Synthetic Chemistry, School of Chemistry, Sun Yat-Sen University, Guangzhou 510275, PR China.
[d] School of Chemical Technology, Guangdong Industry Polytechnic, Guangzhou 510300, PR China.
[e] School of Chemical Engineering and Light Industry, Guangdong University of Technology, Guangzhou 510006, PR China.

‡ Equal contribution.

Methods.

Scheme S1. Synthesis of TPI-based molecules.

Scheme S2. Ionization of TPI-COOH-2OH in the uncharged state.

Scheme S3. Ionization of TPI-COOH-2OH in the zwitterionic state.

Figure S1. The effects of solvent and disturbed push–pull π-electron system on fluorescence emission for a fluorophore with an ICT excited state.

Figure S2. The emission spectra of (a) 100 and (b) 10 μM TPI-COOH-2OH in mixed water/MeCN solutions with different f_w, respectively.

Figure S3. The emission spectra of (a) 100 and (b) 10 μM TPI-COOH-2OH in mixed water/EtOH solutions with different f_w, respectively.

Figure S4. The emission spectra of 10 μM (a) TPI-COOH-2H, (b) TPI-COOH-2F and (c) TPI-COOH-2OH in mixed water/THF solutions with different f_w, respectively.

Figure S5. Photographs of TPI-COOH-2H, TPI-COOH-2F, TPI-COOH-2OH solid and 100 μM TPI-COOH-2OH in THF under the (a) white light and (b) 365 nm UV light.

Figure S6. The original emission spectra of 100 μM TPI-COOH-2OH in mixed water/THF solutions with different f_w.

Figure S7. Photographs of 100 μM TPI-COOH-2OH in mixed water/THF solutions with different f_w, passed through by a beam of red light.

Figure S8. The emission spectra of 1 μM TPI-COOH-2OH in mixed water/THF solutions with different f_w.

Figure S9. The absorption spectra of 100 μM TPI-COOH-2OH in mixed water/THF solutions.

Figure S10. The absorption spectra of 100 μM TPI-COOH-2OH in mixed water/THF solution (f_w = 20%) with different pH.

Figure S11. The absorption spectra of 100 μM TPI-COOH-2OH in mixed water/THF solution (f_w = 90%) with different pH.

Figure S12. The absorption titration curves of 100 μM TPI-COOH-2OH in mixed water/THF solutions when f_w = (a) 20% (absorbance values at 360 nm) and (b) 90% (absorbance values at 290 nm).

Figure S13. (a) The absorption spectra and (b) the corresponding titration curve (pH/Abs$_{366\ nm}$ curve) of 100 μM TPI-COOCH3-2OH in mixed water/THF solution (f_w = 20%) with different pH.

Figure S14. (a) The absorption spectra and (b) the corresponding titration curve (pH/Abs$_{351\ nm}$ curve) of 100 μM TPI-COOCH3-2OH in mixed water/THF solution (f_w = 90%) with different pH.

Figure S15. Molecular orbital diagrams of HOMO and LUMO for the uncharged molecule and the anion of TPI-COOH-2OH at the first excited singlet state.

Figure S16. Photographs of 10 μM TPI-COOH-2OH in mixed (a) ethyl acetate/alcohol and (b) THF/alcohol solutions with different ratios, excited by 365 nm UV light.

Figure S17. The absorption spectra of 100 μM (a) TPI-COOH-2H and (b) TPI-COOH-2F in mixed water/THF solutions (f_w = 0 and 90%).

Figure S18. The structures of TPI-based molecules without carboxyl groups.

Figure S19. The absorption spectra of 100 μM (a) TPI-CN-2H, (b) TPI-CN-2OH, (c) TPI-OH-2F and (d) TPI-OH-2OH in mixed water/THF solutions with different f_w.

Figure S20. The emission spectra of 100 μM (a) TPI-CN-2H, (b) TPI-CN-2OH, (c) TPI-OH-2F and (d) TPI-OH-2OH in mixed water/THF solutions with different f_w.

Figure S21. The decay curves of 100 μM (a) TPI-COOH-2OH, (b) TPI-CN-2OH, (c) TPI-OH-2F and (d) TPI-OH-2OH in mixed water/THF solutions with different f_w.

Eq. S1. Titration equation.

Eq. S2. Adams' equation.

Table S1. Summary of fluorescence variations of TPI-based ampholytes in mixed water/THF solutions.

Table S2. Summary of fluorescence variations of TPI-COOH-2OH in mixed water/MeCN and water/EtOH solutions.

Table S3. The TDDFT results of the uncharged molecule and the anion of TPI-COOH-2OH.

Table S4. Photoluminescence quantum yields of 100 μM TPI-based molecules in dry THF.

Methods

All commercially available reagents and solvents, which were employed for synthesis, were used as received without further purification. The organic solvents for UV–vis absorption and fluorescence measurements were dried by 350 °C-activated molecular sieves.
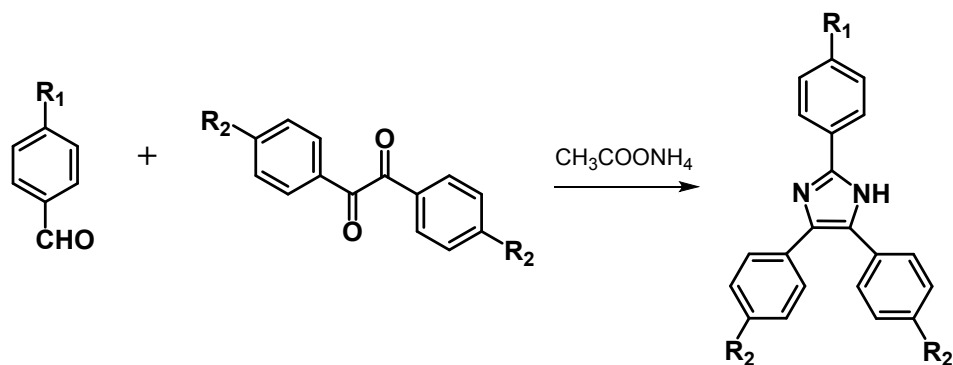
Scheme S1. Synthesis of TPI-based molecules.

Compounds	R_1	R_2
TPI-COOH-2H	COOH	H
TPI-COOH-2F	COOH	F
TPI-COOH-2OH	COOH	OH
TPI-CN-2H	CN	H
TPI-CN-2OH	CN	OH
TPI-OH-2F	OH	F
TPI-OH-2OH	OH	OH
TPI-COOCH3-2OH	COOCH$_3$	OH

TPI-COOH-2OH

A mixture of ammonium acetate (10.0 mmol, 0.770 g), 4-formylbenzoic acid (1.20 mmol, 0.180 g), 1,2-bis(4-hydroxyphenyl)ethane-1,2-dione (1.00 mmol, 0.242 g) and acetic acid (15 mL) were stirred at 110 °C for 10 hours under the protection of nitrogen gas. After reaction, H_2O (10 mL) was added and the mixture was extracted with ethyl acetate. The organic solvent was dried by $MgSO_4$ and then removed under reduced pressure to afford the crude product, which was further purified by column chromatography on silica gel using dichloromethane-methanol (10:1, v/v) to give the product as a yellow solid. Yield = 75%. [1]H nuclear magnetic resonance (^{1}H NMR) (500 MHz, [D_6]DMSO, 298 K, relative to Me_4Si): δ 6.70 (d, J = 8.5 Hz, 2H, phenol), 6.83 (d, J = 8.5 Hz, 2H, phenol), 7.33 (dd, J = 30.0, 8.5 Hz, 4H, phenol), 8.00 (d, J = 8.5 Hz, 2H, phenylbenzoic acid), 8.15 ppm (d, J = 8.5 Hz, phenylbenzoic acid). MS (ESI[−]): m/z: calculated for [M-H][−] 371.11, found 371.17.

The procedures of other TPI derivatives were similar to that for TPI-COOH-2OH.

TPI-COOH-2H

^{1}H NMR (500 MHz, [D_6]DMSO, 298 K, relative to Me_4Si): δ 7.21−7.60 (m, 10H, phenyl), 8.04 (d, J = 8.4 Hz, 2H, phenylbenzoic acid), 8.20 ppm (d, J = 8.4 Hz, 2H, phenylbenzoic acid). Yield = 75%. MS (ESI[−]): m/z: calculated for [M-H][−] 339.12, found 339.17.

TPI-COOH-2F

^{1}H NMR (500 MHz, [D_6]DMSO, 298 K, relative to Me_4Si): δ 7.17 (t, J = 8.9 Hz, 2H, phenyl fluoride), 7.33 (t, J = 8.8 Hz, 2H, phenyl fluoride), 7.51−7.59 (m, 4H, phenyl fluoride), 8.04 (d, J = 8.5 Hz, 2H, phenylbenzoic acid), 8.18 ppm (d, J = 8.5 Hz, 2H, phenylbenzoic acid). Yield = 65%. MS (ESI[−]): m/z: calculated for [M-H][−] 375.10, found 375.00.

TPI-CN-2H

^{1}H NMR (500 MHz, [D_6]DMSO, 298 K, relative to Me_4Si): δ 7.22−7.60 (m, 10H, phenyl), 7.95 (d, J = 8.4 Hz, 2H, phenyl acetonitrile), 8.25 ppm (d, J = 8.5 Hz, 2H, phenyl acetonitrile). Yield = 65%. MS (ESI[−]): m/z: calculated for [M-H][−] 320.13, found 320.25.

TPI-CN-2OH

^{1}H NMR (500 MHz, [D$_6$]DMSO, 298 K, relative to Me$_4$Si): δ 6.76 (dd, J = 64.9, 8.0 Hz, 4H, phenol), 7.32 (d, J = 26.9, 7.9 Hz, 4H, phenol), 7.91 (d, J = 8.5 Hz, 2H, phenyl acetonitrile), 8.20 ppm (d, J = 8.5 Hz, 2H, phenyl acetonitrile). Yield = 70%. MS (ESI$^-$): m/z: calculated for [M-H]$^-$ 352.12, found 352.25.

TPI-OH-2F

^{1}H NMR (500 MHz, [D$_6$]DMSO, 298 K, relative to Me$_4$Si): δ 6.84 (d, J = 8.4 Hz, 2H, phenol), 7.14 (t, J = 8.7 Hz, 2H, phenyl fluoride), 7.29 (t, J = 8.7 Hz, 2H, phenyl fluoride), 7.46−7.56 (m, 4H, phenyl fluoride), 7.87 (d, J = 8.4 Hz, 2H, phenol) ppm. Yield = 55%. MS (ESI$^-$): m/z: calculated for [M-H]$^-$ 347.11, found 347.25.

TPI-OH-2OH

^{1}H NMR (500 MHz, [D$_6$]DMSO, 298 K, relative to Me$_4$Si): δ 6.66−6.80 (s, 4H, 4,5-phenol), 6.83 (d, J = 7.8 Hz, 2H, 2-phenol), 7.30 (d, J = 7.7 Hz, 4H, 4, 5-phenol), 7.85 ppm (d, J = 7.9 Hz, 2H, 2-phenol). Yield = 55%. MS (ESI$^-$): m/z: calculated for [M-H]$^-$ 343.12, found 343.17.

TPI-COOCH3-2OH

^{1}H NMR (500 MHz, [D$_6$]DMSO, 298 K, relative to Me$_4$Si): δ 3.85−3.90 (s, 3H, CH$_3$), 6.70 (d, J = 8.2 Hz, 2H, phenol), 6.82 (d, J = 8.1 Hz, 2H, phenol), 7.33 (dd, J = 30.2, 8.1 Hz, 4H, phenol), 8.03 (d, J = 8.4 Hz, 2H, phenyl ester), 8.18 ppm (d, J = 8.4 Hz, 2H, phenyl ester). Yield = 75%. MS (ESI$^+$): m/z: calculated for [M+H]$^+$ 387.13, found 387.25.

Instruments. The ^{1}H NMR measurements were performed on a Bruker Ascend NMR spectrometer operated at 500 MHz. UV-vis absorption spectra were recorded on a Shimadzu UV−2600 UV−vis absorption spectrometer. Fluorescence emission spectra were recorded by Edinburgh FS5 fluorescence spectrometer equipped with a continuous Xe lamp. The fluorescence lifetime experiments were performed by the Edinburgh FLS980 fluorescence spectrometer equipped with 340 or 369 nm picosecond pulsed diode lasers as the excitation source. The photoluminescence quantum yield (PLQY) measurements were performed by the Quantaurus-QY (Hamamatsu, Japan) in the integrating sphere. The estimated experimental error for PLQYs determination was 1%. The mass spectra were record by a Thermo Scientific LCQ Fleet mass spectrometer equipped with ESI source. DLS measurements were performed on a Microtrac/Nanotrac Wave II DLS particle size/zeta potential analyzer.

The HCl and NaOH aqueous solutions were used to adjust the pH, and the pH was record by a pH meter (LONTROL, China) in the titration experiment.

Density functional theory (DFT) calculations. DFT calculations were performed using Gaussian 09 program[S1]. Geometry optimization were performed using by CAM-B3LYP density function and the 6-31G++ (d, p) basis set for all the molecules. The SMD solvation model was used to perform geometry optimization in THF and water for the uncharged molecule and the anion, respectively.

Time-dependent density functional theory (TDDFT) calculations. TDDFT calculations were used to investigate the photophysical differences of the uncharged molecule and the anion. Calculations were performed with the same function and basis set as described for the DFT optimizations.
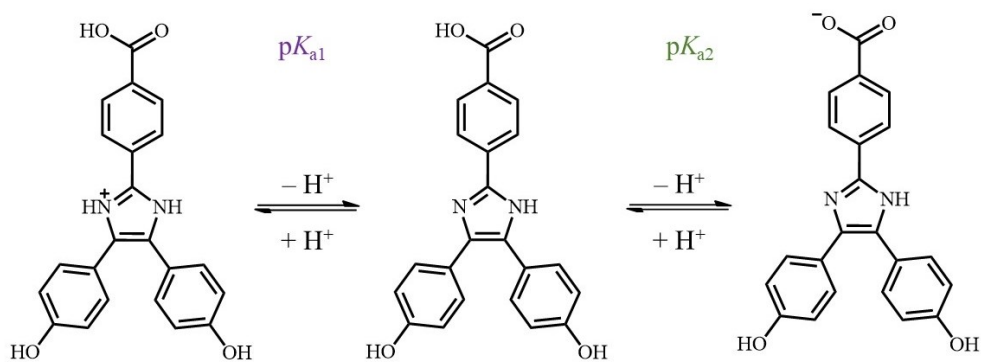
Scheme S2. Ionization of TPI-COOH-2OH in the uncharged state.
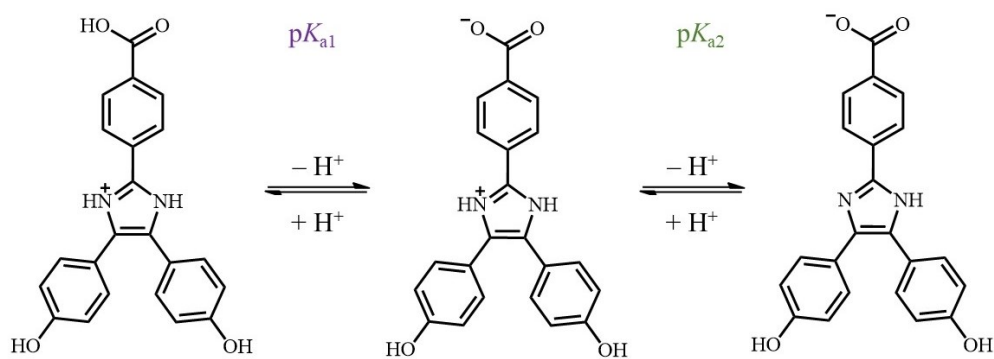
Scheme S3. Ionization of TPI-COOH-2OH in the zwitterionic state.
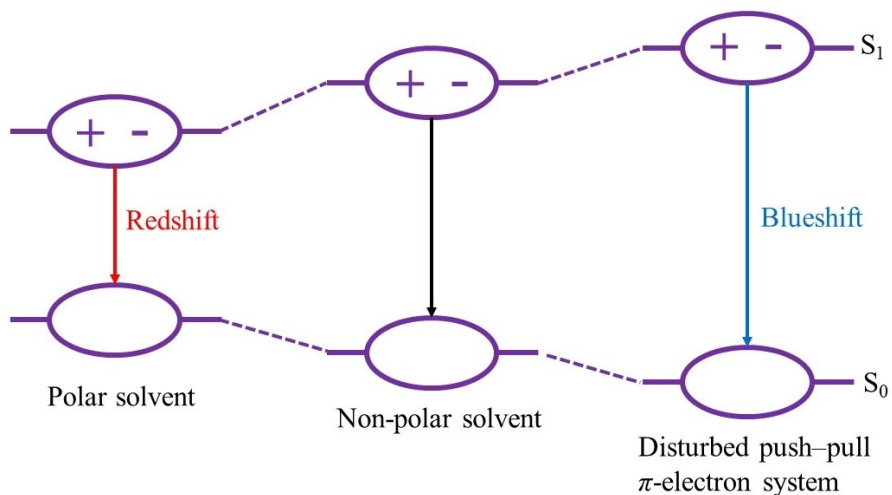
Figure S1. The effects of solvent and disturbed push–pull π-electron system on fluorescence emission for a fluorophore with an ICT excited state. S_0 and S_1 represent the singlet electronic ground and lowest energy excited states, respectively.
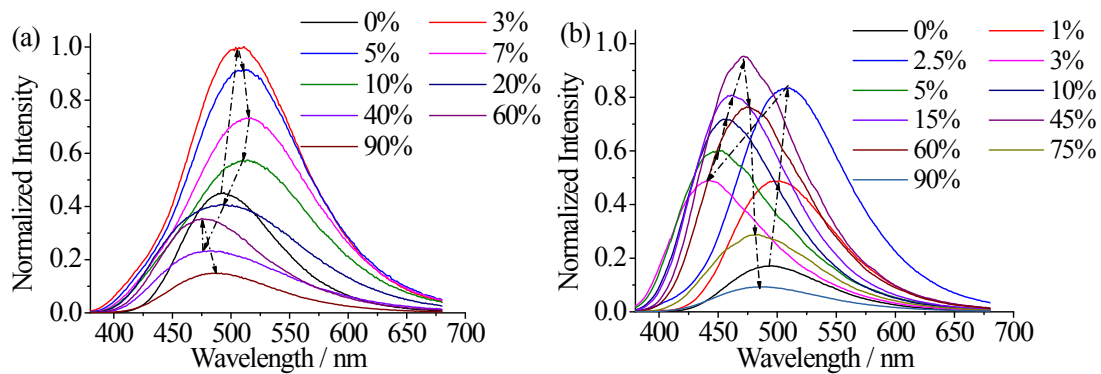
Figure S2. The emission spectra of (a) 100 and (b) 10 μM TPI-COOH-2OH in mixed water/MeCN solutions with different f_w, respectively.

Figure S3. The emission spectra of (a) 100 and (b) 10 μM TPI-COOH-2OH in mixed water/EtOH solutions with different f_w, respectively.

Figure S4. The emission spectra of 10 μM (a) TPI-COOH-2H, (b) TPI-COOH-2F and (c) TPI-COOH-2OH in mixed water/THF solutions with different f_w, respectively.

(a)

(b)
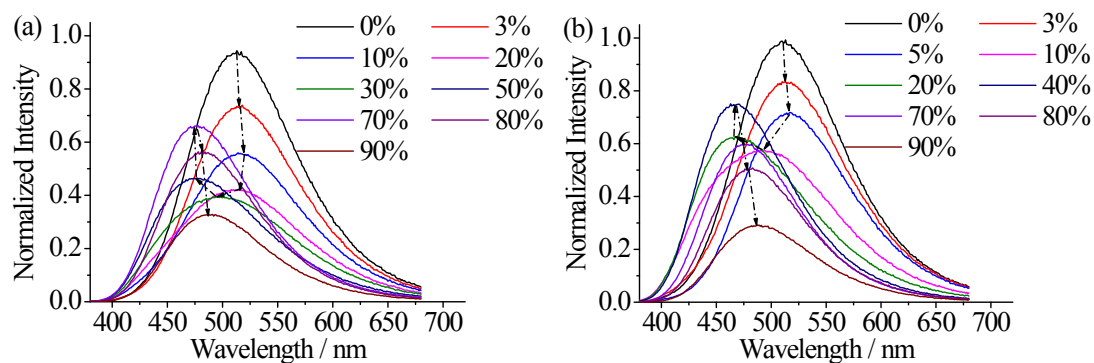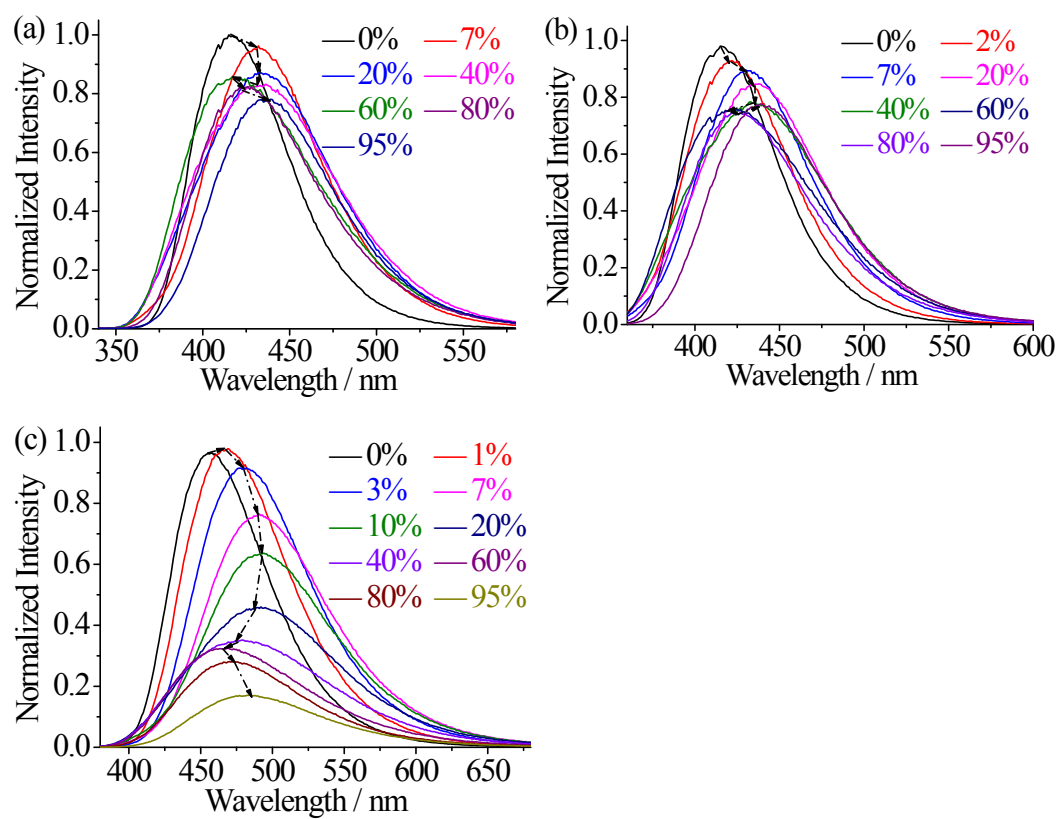
Figure S5. Photographs of TPI-COOH-2H, TPI-COOH-2F, TPI-COOH-2OH solid and 100 μM TPI-COOH-2OH in THF (from left to right) under the (a) white light and (b) 365 nm UV light, respectively.
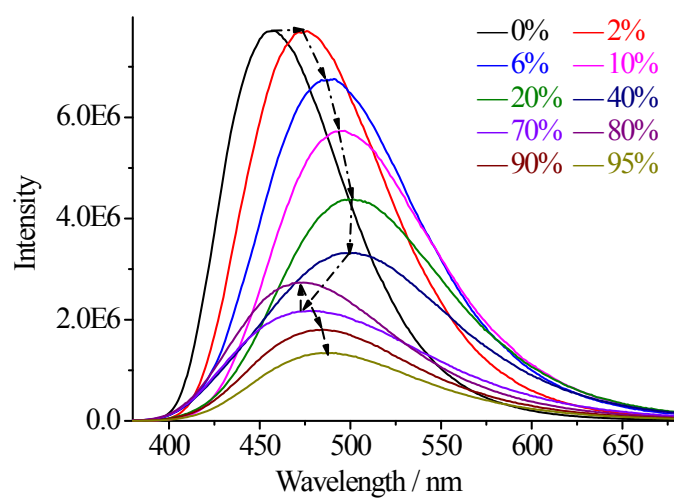
Figure S6. The original emission spectra of 100 μM TPI-COOH-2OH in mixed water/THF solutions with different f_w.
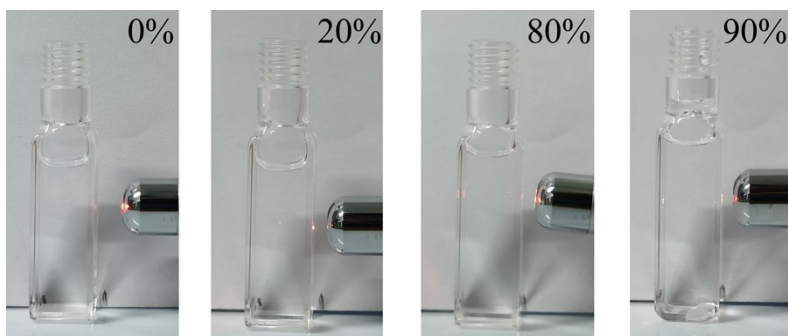
Figure S7. Photographs of 100 µM TPI-COOH-2OH in mixed water/THF solutions with different f_w, passed through by a beam of red light.
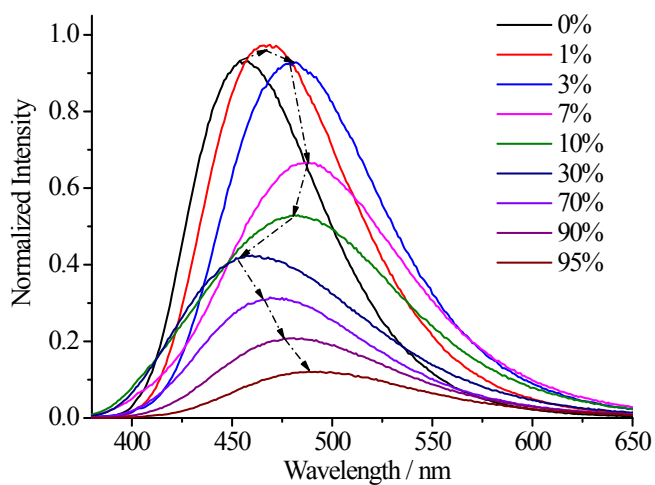

Figure S8. The emission spectra of 1 µM TPI-COOH-2OH in mixed water/THF solutions with different f_w.
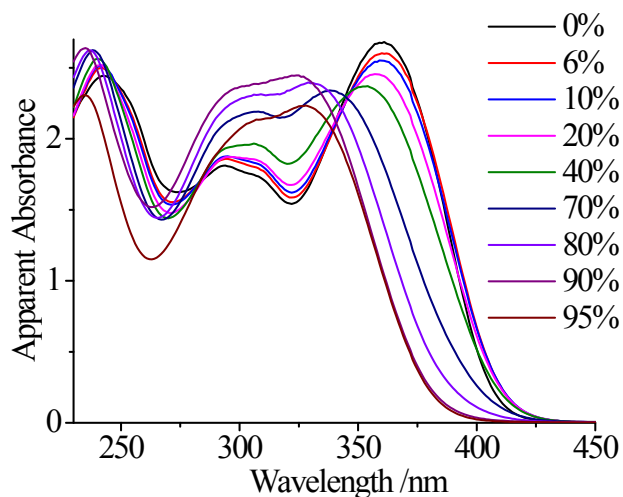
Figure S9. The absorption spectra of 100 μM TPI-COOH-2OH in mixed water/THF solutions with different f_w.
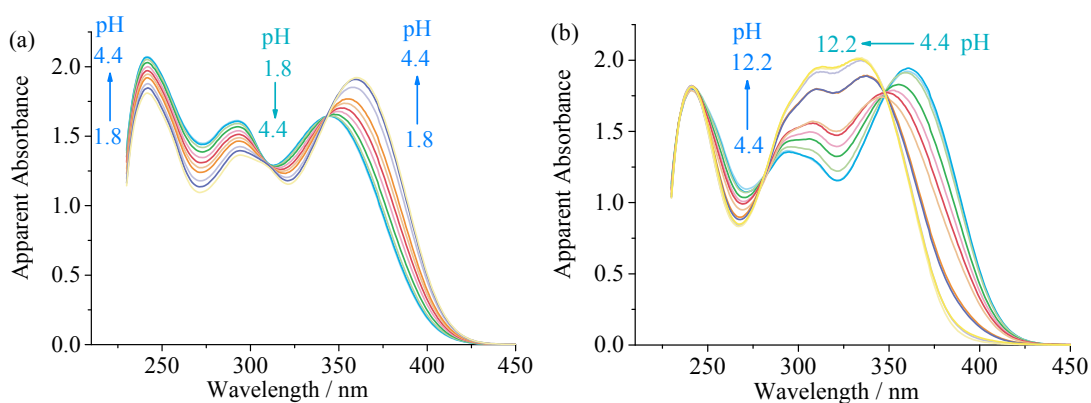

Figure S10. The absorption spectra of 100 μM TPI-COOH-2OH in mixed water/THF solution ($f_w = 20\%$) with different pH.
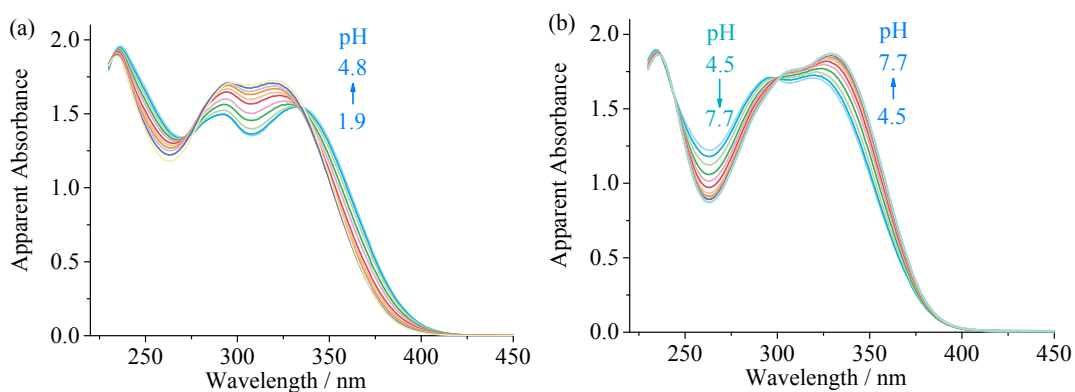

Figure S11. The absorption spectra of 100 μM TPI-COOH-2OH in mixed water/THF solution ($f_w = 90\%$) with different pH.
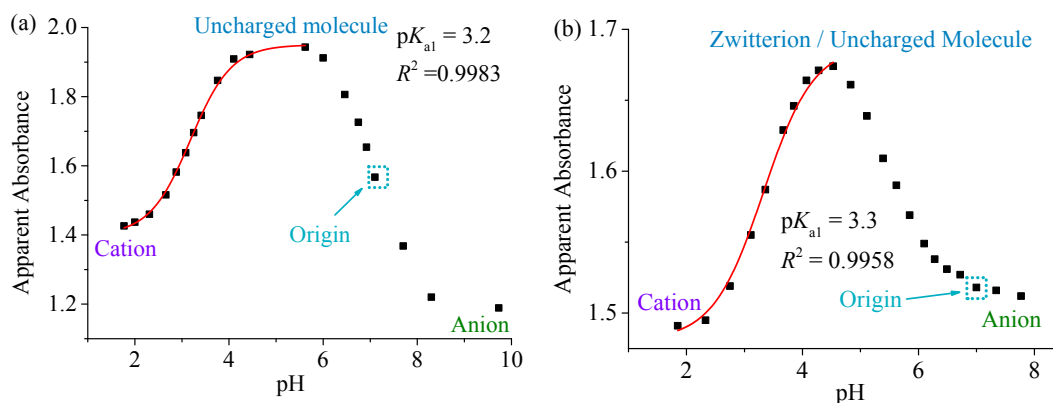
Figure S12. The absorption titration curves of 100 μM TPI-COOH-2OH in mixed water/THF solutions when f_w = (a) 20% (absorbance values at 360 nm) and (b) 90% (absorbance values at 290 nm).
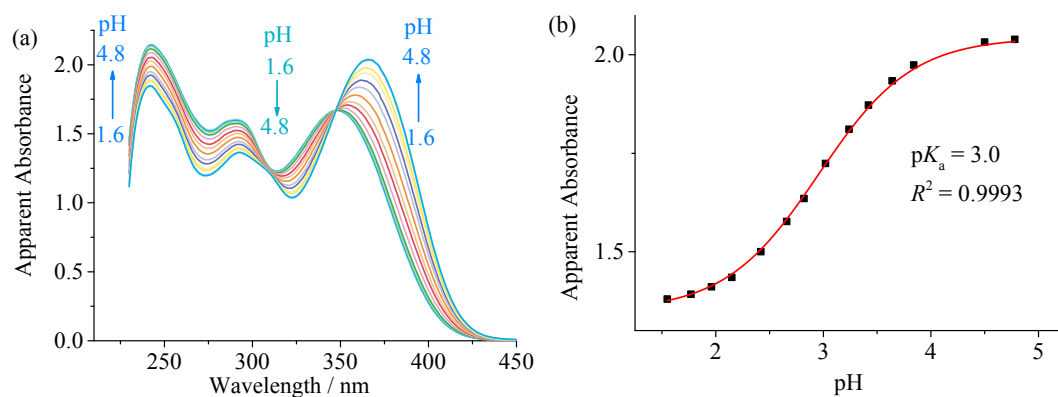

Figure S13. (a) The absorption spectra and (b) the corresponding titration curve (pH/Abs$_{366\,nm}$ curve) of 100 μM TPI-COOCH3-2OH in mixed water/THF solution (f_w = 20%) with different pH.
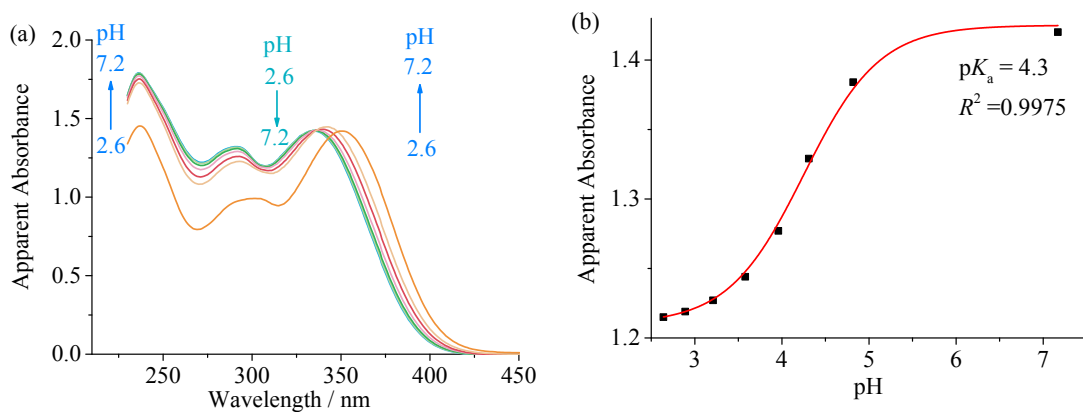
Figure S14. (a) The absorption spectra and (b) the titration curve (pH/$Abs_{351\ nm}$ curve) of 100 µM TPI-COOCH3-2OH in mixed water/THF solution ($f_w = 90\%$) with different pH.

Uncharged molecule
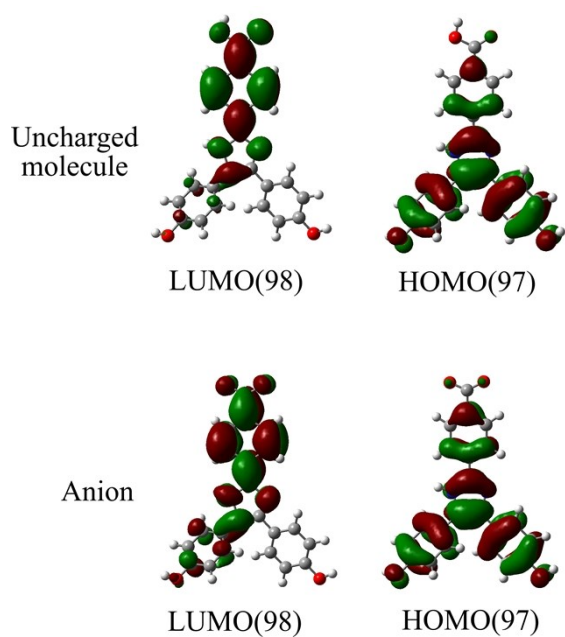
LUMO(98) HOMO(97)

Anion

LUMO(98) HOMO(97)

Figure S15. Molecular orbital diagrams of HOMO and LUMO for the uncharged molecule and the anion of TPI-COOH-2OH at the first excited singlet state. 98 and 97 mean the sequence number of the molecular orbital.
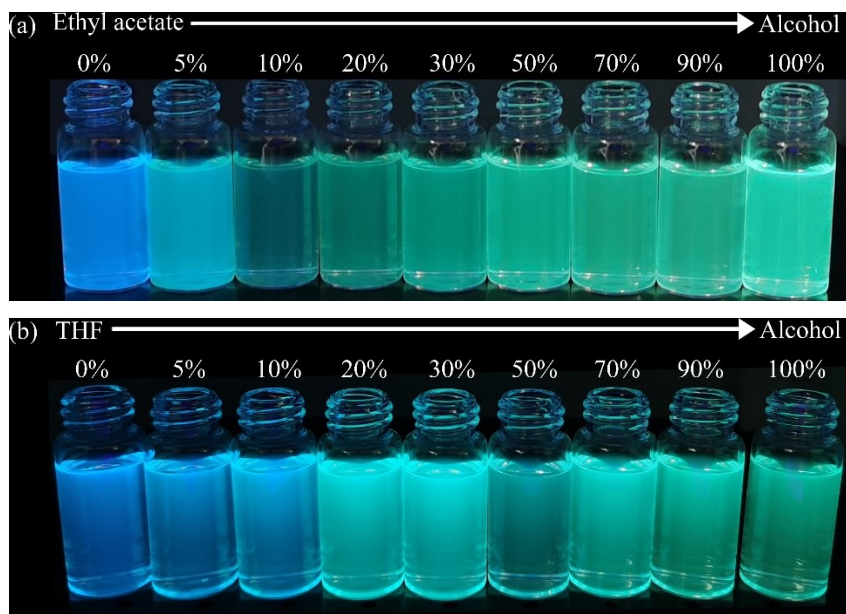
Figure S16. Photographs of 10 μM TPI-COOH-2OH in mixed (a) ethyl acetate/alcohol and (b) THF/alcohol solutions with different ratios, excited by 365 nm UV light.
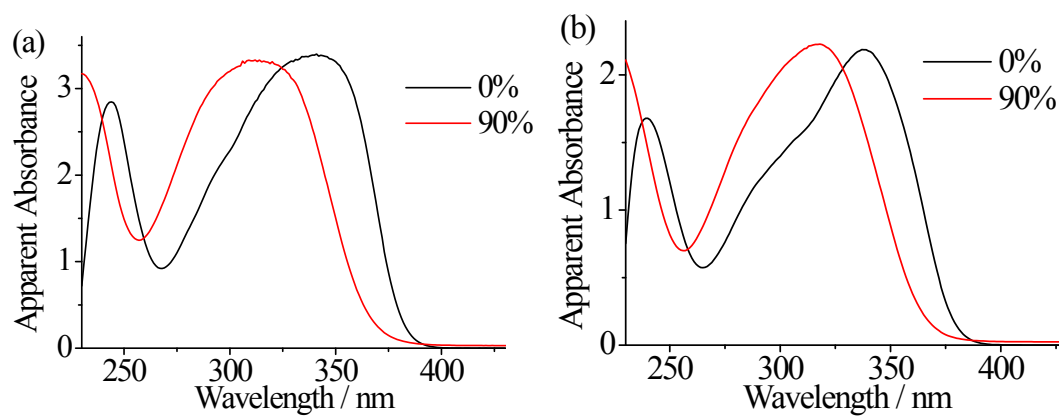

Figure S17. The absorption spectra of 100 μM (a) TPI-COOH-2H and (b) TPI-COOH-2F in mixed water/THF solutions (f_w = 0 and 90%).
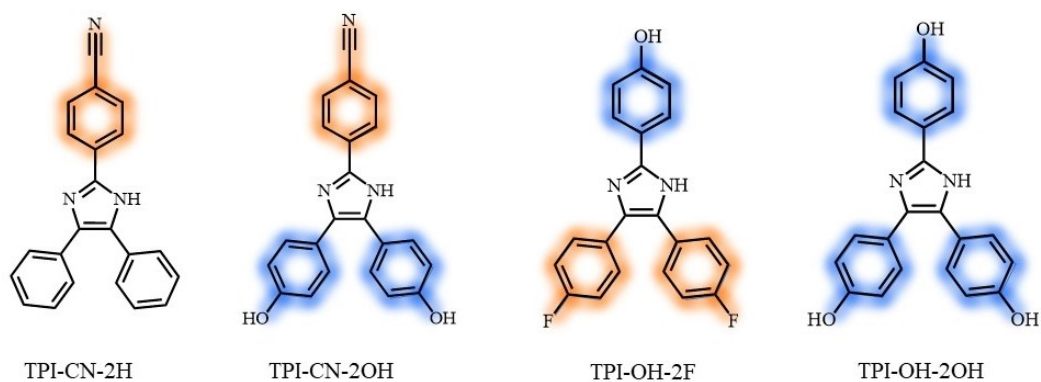
Figure S18. The structures of TPI-based molecules without carboxyl groups. Blue shading: electron-donating groups; orange shading: electron-withdrawing groups.
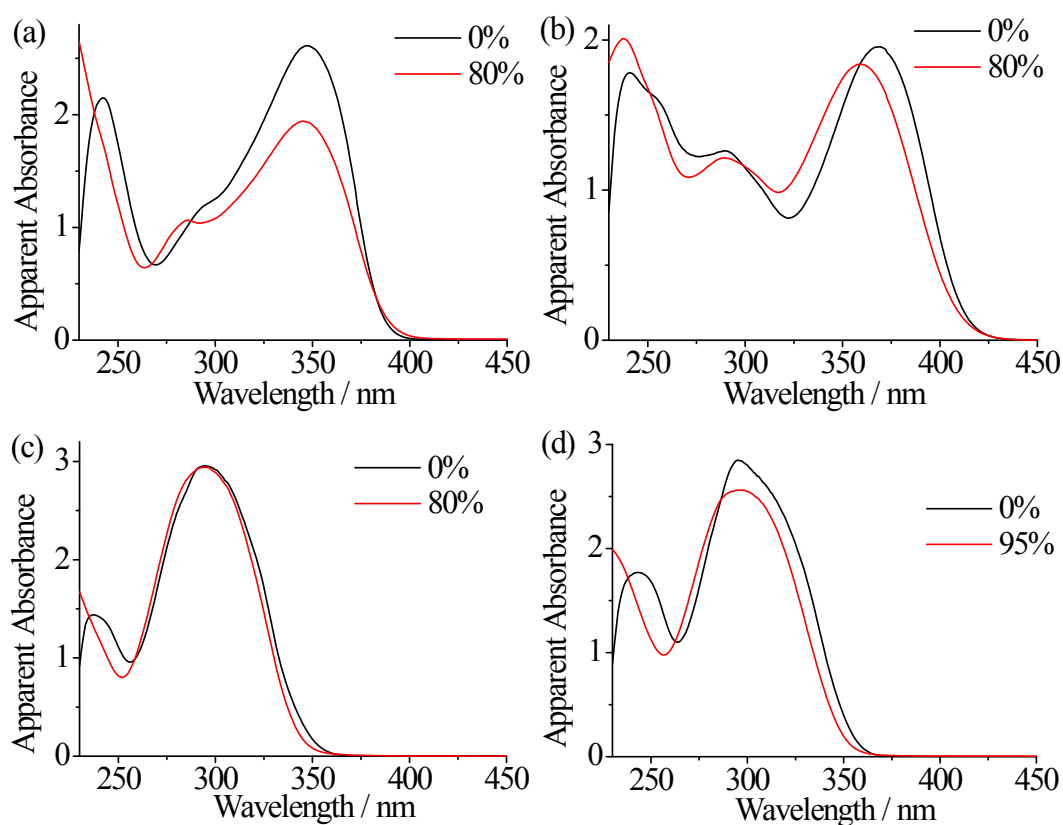

Figure S19. The absorption spectra of 100 μM (a) TPI-CN-2H, (b) TPI-CN-2OH, (c) TPI-OH-2F and (d) TPI-OH-2OH in mixed water/THF solutions with different f_w.
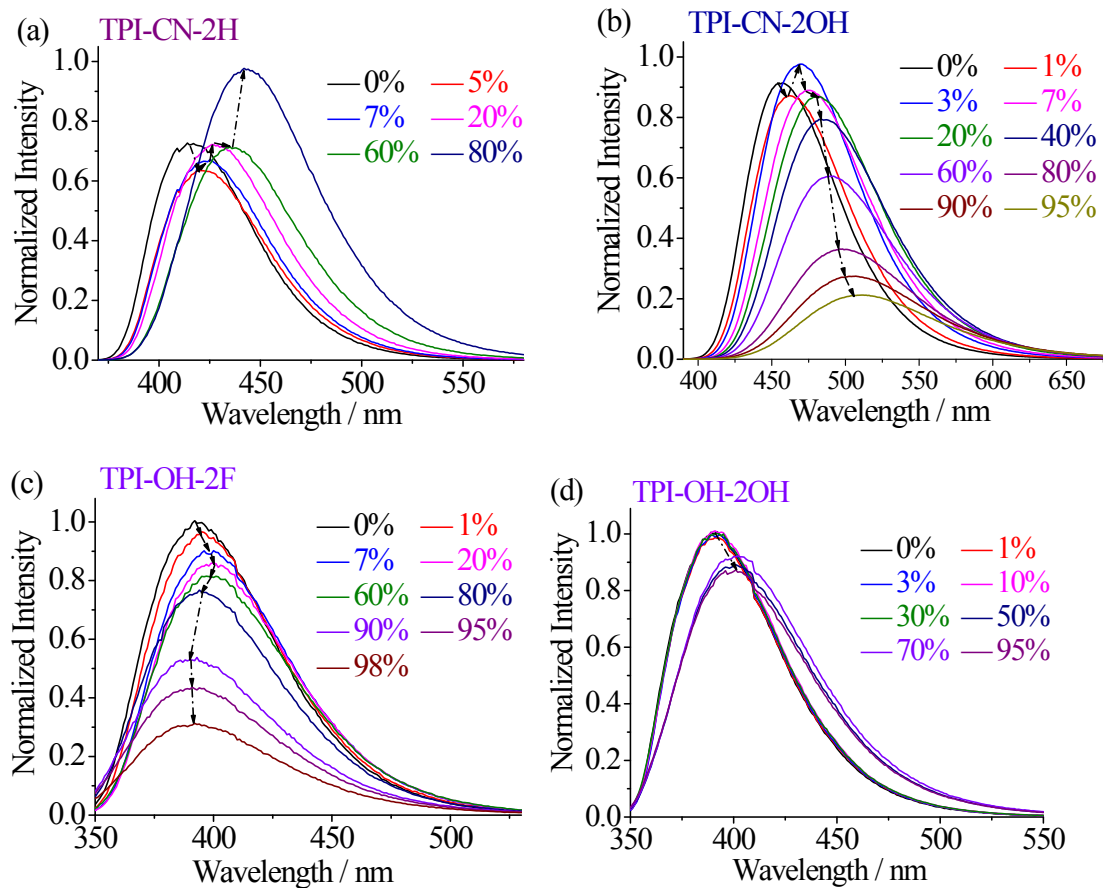
Figure S20. The emission spectra of 100 μM (a) TPI-CN-2H, (b) TPI-CN-2OH, (c) TPI-OH-2F and (d) TPI-OH-2OH in mixed water/THF solutions with different f_w.
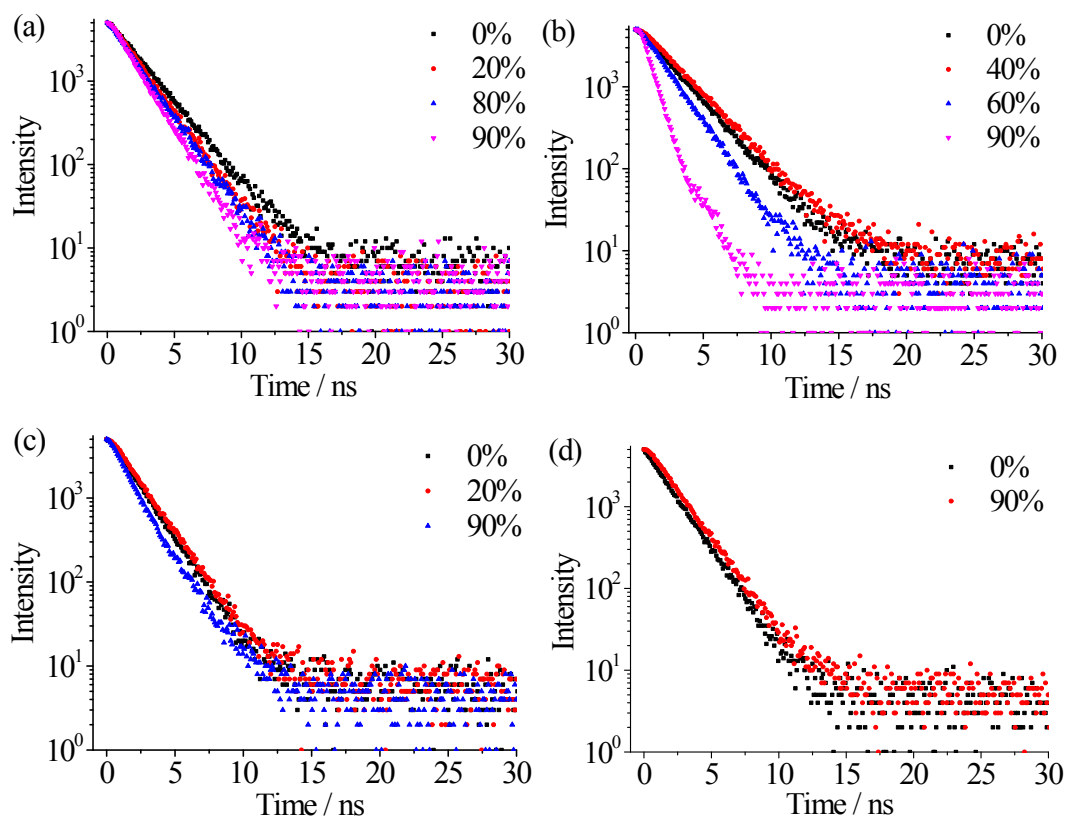
Figure S21. The decay curves of 100 μM (a) TPI-COOH-2OH, (b) TPI-CN-2OH, (c) TPI-OH-2F and (d) TPI-OH-2OH in mixed water/THF solutions with different f_w, excited by lasers.

Titration equation

$$pK_a = \lg(A_I - A)/(A - A_N) + pH \quad \text{(Eq. S1)}$$

A_I and A_N represent the absorbance when the compounds all in the anion state and the neutral state, respectively. And the A represent the corresponding absorbance values in different pH.

Adams' equation[S2]

$$K_z = K_a^A / K_a^E - 1 \quad \text{(Eq. S2)}$$

K_z represents tautomeric equilibrium constant defined as the ratio of concentrations of the zwitterionic and uncharged forms. K_a^A represents macrodissociation constant associated with the stoichiometric equilibria of an ampholyte. It denotes the loss of the first proton from the molecule dissociation constant of the cation/zwitterion equilibrium. K_a^E represents dissociation constant associated with the stoichiometric equilibria of the corresponding ester to the ampholyte.）

For example,

When $f_w = 20\%$,

pK_{a1} (TPI-COOH-2OH) = 3.0, pK_{a1} (TPI-COOCH3-2OH) = 3.2,

$K_z = K_a^A / K_a^E - 1 = K_{a1}$ (TPI-COOH-2OH) / K_{a1} (TPI-COOCH3-2OH) – 1= $10^{-3.2}/10^{-3.0} - 1 = -0.37$,

n(zwitterion) / n(uncharged molecule) ≈ 0.

When $f_w = 90\%$,

pK_{a1} (TPI-COOH-2OH) = 3.3, pK_{a1} (TPI-COOCH3-2OH) = 4.3,

$K_z = K_a^A / K_a^E - 1 = K_{a1}$ (TPI-COOH-2OH) / K_{a1} (TPI-COOCH3-2OH) – 1= $10^{-3.3}/10^{-4.3} - 1 = 9$,

n(zwitterion) / n(uncharged molecule) ≈ 9.

Table S1. Summary of fluorescence variations of TPI-based ampholytes in mixed water/THF solutions.

Molecule	c / μM	State 1 λ_{max}, f_w	State 2 λ_{max}, f_w	State 3 λ_{max}, f_w	State 4 λ_{max}, f_w
TPI-COOH-2H	100	416 nm, 0%	450 nm, 60%	428 nm, 95%	/
	10	416 nm, 0%	433 nm, 20%	416 nm, 60%	436 nm, 95%
TPI-COOH-2F	100	416 nm, 0%	453 nm, 60%	433 nm, 90%	/
	10	416 nm, 0%	436 nm, 20%	421 nm, 60%	439 nm, 95%
TPI-COOH-2OH	100	456 nm, 0%	501 nm, 20%	471 nm, 80%	486 nm, 95%
	10	456 nm, 0%	492 nm, 10%	463 nm, 60%	486 nm, 95%
	1	456 nm, 0%	480 nm, 3%	456 nm, 30%	488 nm, 95%

Table S2. Summary of fluorescence variations of TPI-COOH-2OH in mixed water/MeCN and water/EtOH solutions.

Solution	c/μM	State 1 λ_{max}, f_w	State 2 λ_{max}, f_w	State 3 λ_{max}, f_w	State 4 λ_{max}, f_w
Water/MeCN	100	493 nm, 0%	515 nm, 7%	475 nm, 60%	486 nm, 90%
	10	493 nm, 0%	508 nm, 2.5%	441 nm, 3%	486 nm, 90%
Water/EtOH	100	512 nm, 0%	517 nm, 10%	476 nm, 50%	487 nm, 90%
	10	512 nm, 0%	517 nm, 5%	467 nm, 20%	487 nm, 90%

Table S3. The TDDFT results of the uncharged molecule and the anion of TPI-COOH-2OH.

Ionic species	Excited state	Configuration (CI coefficient)	λ/nm	E/eV	f^a
Uncharged molecule	1	97 to 98 (0.662)	340	3.65	0.930
Anion	1	97 to 98 (0.655)	314	3.95	0.829

[a] Oscillator strength.

Table S4. Photoluminescence quantum yields of 100 μM TPI-based molecules in dry THF.

Molecules	PLQY
TPI-COOH-2OH	69%
TPI-COOH-2H	74%
TPI-COOH-2F	78%
TPI-CN-2H	67%
TPI-CN-2OH	73%
TPI-F-2OH	34%
TPI-OH-2OH	48%

Supplementary References

[S1] M. J. Frisch, G. W. Trucks, H. B. Schlegel, G. E. Scuseria, M. A. Robb, J. R. Cheeseman, G. Scalmani, V. Barone, B. Mennucci, G. A. Petersson, H. Nakatsuji, M. Caricato, X. Li, H. P. Hratchian, A. F. Izmaylov, J. Bloino, G. Zheng, J. L. Sonnenberg, M. Hada, M. Ehara, K. Toyota, R. Fukuda, J. Hasegawa, M. Ishida, T. Nakajima, Y. Honda, O. Kitao, H. Nakai, T. Vreven, J. A. Montgomery Jr, J. E. Peralta, F. Ogliaro, M. Bearpark, J. J. Heyd, E. Brothers, K. N. Kudin, V. N. Staroverov, R. Kobayashi, J. Normand, K. Raghavachari, A. Rendell, J. C. Burant, S. S. Iyengar, J. Tomasi, M. Cossi, N. Rega, J. M. Millam, M. Klene, J. E. Knox, J. B. Cross, V. Bakken, C. Adamo, J. Jaramillo, R. Gomperts, R. E. Stratmann, O. Yazyev, A. J. Austin, R. Cammi, C. Pomelli, J. W. Ochterski, R. L. Martin, K. Morokuma, V. G. Zakrzewski, G. A. Voth, P. Salvador, J. J. Dannenberg, S. Dapprich, A. D. Daniels, O. Farkas, J. B. Foresman, J. V. Ortiz, J. Cioslowski and D. J. Fox, *Gaussian, Inc.*, Wallingford CT, 2009.

[S2] A. Pagliara, P.-A. Carrupt, G. Caron, P. Gaillard, and B. Testa, *Chem. Rev.* 1997, **97,** 3385-3400.